Co-fan-sum ratio algorithm for randoms smoothing and detector normalization in PET

Charles C. Watson, *Senior Member, IEEE*

***Abstract*—We describe a new exact analytical algorithm for estimating the single event rates in detectors from random coincidence data (for randoms variance reduction), and detector efficiencies from true coincidence data (for normalization), in positron emission tomography (PET). The estimates are derived from the ratios of the co-fan sums of coincidence events between individual detectors. The co-fan for any two detectors is defined as the set of co-detectors they have in common among the measured lines of response. The estimates are unbiased and have noise properties similar to fan-sum estimates. The detector efficiency estimation algorithm additionally employs the concept of a mask-restricted co-fan sum that can be easily adapted to a known source distribution, and thus does not require uniform illumination of all lines of response, or a centered uniform cylindrical source, for accurate estimation. The algorithm is simple to implement and can be applied in 2D or 3D. Some examples are given.**

I. Introduction

Random coincidence rates in PET are approximately related to detector single event rates according to:

$$R_{ij} = 2\tau s_i s_j \,, \tag{1}$$

where R_{ij} is an element of a delayed coincidence sinogram corresponding to detectors i and j, s_i and s_j are their corresponding singles rates, and 2τ is the coincidence time window. Although this expression neglects the effect of true coincidence singles, multiplexing losses, and other factors [1], it is widely used as the basis of most randoms variance reduction algorithms.

True coincidence rates can be approximately related to detector efficiencies in a mathematically similar way. Let T_{ij} be an element of a trues (prompt - delayed coincidence) sinogram corresponding to detectors i and j. If the sinogram has been corrected for geometrical efficiency variations, and time alignment and dead time effects are neglected, then the trues rate is related to the intrinsic efficiencies ϵ_i and ϵ_j of the detectors by:

$$T_{ij} = \epsilon_i \epsilon_j \, t_{ij} \,, \tag{2}$$

where t_{ij} is the incident photon flux along the ij line of response (LOR). The variation of the t_{ij} factors is sometimes neglected under the assumption that their effect averages out. In this case, the efficiency and singles estimation problems would be mathematically equivalent. In general the t_{ij} factors can vary significantly, however, and this may not be a good approximation.

Manuscript received November 13, 2010.

The author is with Siemens Healthcare Molecular Imaging, Knoxville, TN 37932 USA (telephone: 865.218.2419, e-mail: charles.c.watson@siemens.com)

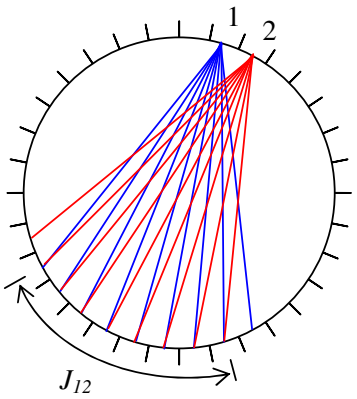

Fig. 1. The intersection of the fans of two detectors defines their co-fan.

Since there are many more LORs than detectors, the above relations can be used to make low-variance estimates of the s_i and ϵ_i from the measured coincidence data, and these in turn can be used to make low-variance estimates of the randoms and normalization factors needed for PET data corrections. Analytical [2], [3], [4], iterative [5] and combination [6] techniques have been developed for estimating the s_i or ϵ_i. These algorithms may be either exact (unbiased) or approximate. Existing exact analytical algorithms [2] and [4] do not necessarily make use of all available data, and thus may produce noisier estimates than the approximate fan-sum algorithm (FSA) of Hoffman et al. [3], which does. These analytical algorithms also neglect the effect of data compression (summation of native physical LORs into virtual LORs). Iterative algorithms, on the other hand, can employ all available data, and account for data compression [7], but may require regularization [8], which can potentially produce bias.

We propose a new exact analytical algorithm that has some similarity to both the FSA and the algorithm of Defrise et al. [4]. It has the advantages that it is conceptually simple, very fast to compute, and uses nearly all available data for the estimates. It is unbiased when applied to uncompressed (native LOR) data, that is, when (1) and (2) are exact. It can be applied in 2D (within a detector ring) or in 3D (both within and across detector rings). The discussion and examples in this paper are for the 2D implementation.

II. Methods

A. Estimating singles rates from randoms

Consider two adjacent individual detectors, i_1 and i_2 in a ring of detectors as shown in Fig. 1. The "fans" of these detectors (i.e., the set of all opposing detectors measured in

coincidence with the given detector) will typically overlap nearly completely, as shown. Let J_{12} be the set of opposing detectors common to both fans. We call this the "co-fan" of i_1, i_2. The co-fan sums of i_1 and i_2 are formed by summing the random coincidence data on all LORs between these detectors and their co-fan:

$$\begin{aligned} R_1^{(12)} &= \sum_{j' \in J_{12}} R_{1j'} = 2\tau s_1 \sum_{j' \in J_{12}} s_{j'} \\ R_2^{(12)} &= \sum_{j' \in J_{12}} R_{2j'} = 2\tau s_2 \sum_{j' \in J_{12}} s_{j'} \end{aligned} \quad (3)$$

where the superscript (12) refers to the co-fan. Taking the ratio of these co-fan sums, the sums over the singles rates in the opposing detectors cancel exactly (except for noise), and we have an unbiased estimate of the ratio of the singles rates in the two detectors:

$$\left(\frac{s_2}{s_1}\right)_{est} = \frac{R_2^{(12)}}{R_1^{(12)}} \quad (4)$$

A key difference between this and the FSA is that in the latter the sums are over the detectors' fans rather than their co-fans, and the variation in these fan sums is neglected, leading to bias.

Suppose there are n detectors in the ring, numbered sequentially. The set of $n-1$ co-fan-sum ratios of adjacent pairs

$$\frac{R_2^{(12)}}{R_1^{(12)}}, \frac{R_3^{(23)}}{R_2^{(23)}}, \ldots, \frac{R_n^{((n-1)n)}}{R_{n-1}^{((n-1)n)}} \quad (5)$$

is sufficient to estimate the ratio of the singles rates between any two detectors, by multiplying together the appropriate combination of them. In applications of these algorithms, only these relative values are important because the s_i (or ϵ_i) are eventually scaled by a global constant to match the total measured randoms (or a mean detector efficiency of 1). The co-fan-sum ratio (CFSR) algorithm for singles rate estimation and randoms variance reduction in its simplest form is thus:

$$\begin{aligned} \hat{s}_1 &= 1 \\ \hat{s}_i &= \hat{s}_{i-1} \frac{R_i^{((i-1)i)}}{R_{i-1}^{((i-1)i)}}, \; 1 < i \le n \\ \hat{R}_{ij} &= 2\tau(\alpha\hat{s}_i)(\alpha\hat{s}_j) \end{aligned} \quad (6)$$

where α is a constant that is determined by normalization to the measured randoms:

$$\alpha^2 = \frac{\sum_i \sum_{j \in J_i} R_{ij}}{\sum_i \sum_{j \in J_i} 2\tau \hat{s}_i \hat{s}_j} \quad (7)$$

In the FSA algorithm, the singles rates are estimated as proportional to the fan sums, while in the CFSR algorithm the *ratio* of singles rates is estimated as proportional to the *ratio* of their co-fan sums. The relative variance of this ratio is only slightly larger than we would get from the fan-sum technique since the co-fans are only slightly smaller than the total fans. Moreover, the CFSRs in (5) are statistically highly correlated because the left and right co-fans of a given detector are nearly the same. Thus noise does not propagate in the multiplication of the ratios to the extent it would if they were statistically independent.

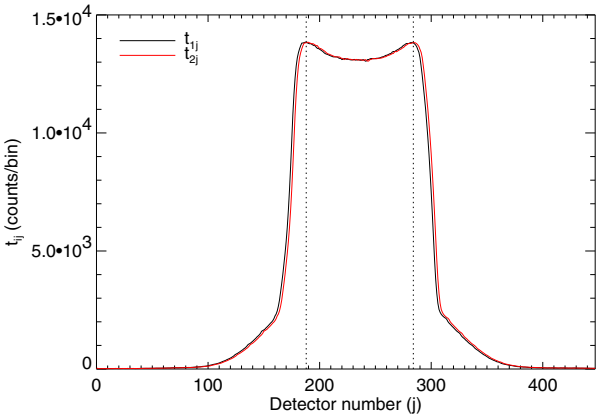

Fig. 2. Typical fan profiles of t_{ij} for two adjacent detectors, for a 20 cm diameter uniform cylindrical source, showing the proposed mask region between the vertical dotted lines.

B. Detector efficiency estimation from trues

The estimation of detector efficiencies from true coincidences is complicated by the presence of the t_{ij} factor in (2). It's not possible to uniformly illuminate all LORs simultaneously with true coincidences using a single source distribution in a ring scanner so that t_{ij} is constant. Typically a a 20 cm diameter cylinder with uniform activity concentration is used as a detector efficiency normalization source. This results in a very non-uniform t_{ij} distribution as shown in Fig. 2. If these t_{ij} factors were neglected, the relative error in the co-fan-sum efficiency ratio estimate would be

$$\frac{(\epsilon_2/\epsilon_1)_{est}}{(\epsilon_2/\epsilon_1)_{true}} - 1 = \frac{\sum_{j \in J_{12}} \epsilon_j \, (t_{2j} - t_{1j})}{\sum_{j \in J_{12}} \epsilon_j \, t_{1j}} \quad (8)$$

For the 20 cm cylinder, $|t_{2j} - t_{1j}|$ is very small except where the profile is changing rapidly at the edges of the phantom. Therefore, by restricting the co-fan sums to a region near the center of the phantom's profile, where t_{ij} is nearly constant, the error due to neglect of the t_{ij} can be made negligible, and essentially the same algorithm described above can be used to estimate the ϵ_i:

$$\left(\frac{\epsilon_2}{\epsilon_1}\right)_{est} \approx \frac{T_2^{(12)mask}}{T_1^{(12)mask}} \quad (9)$$

where

$$T_1^{(12)mask} = \sum_{j' \in J_{12}^{mask}} T_{1j'} \quad (10)$$

etc., and J_{12}^{mask} is the co-fan of detectors 1 and 2 within a masked region of the emission sinogram defined so that t_{ij} is only slowly varying within it. It is beneficial that this masked region excludes much of the scattered coincidence data from the estimate. Another advantage of this approach is that it does not require an accurate model of the t_{ij} to correct the data. Further, the masked co-fan-sum approach can be easily applied to off-center cylinders or other phantoms, making it insensitive to the phantom's position, unlike the fan-sum algorithm.

Fig. 3. Phantom configuration for randoms smoothing example.

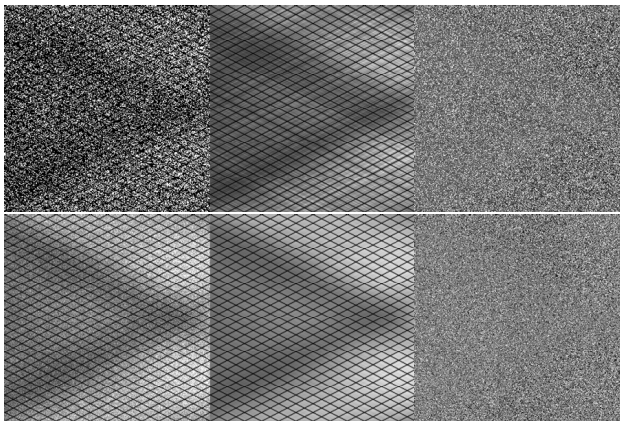

Fig. 4. Delayed coincidence sinograms with a mean of 0.44 counts/bin (Top) and 22 counts/bin (Bottom). Left to Right: Measured, Smoothed, Difference.

The mask-restricted co-fan-sum ratio algorithm for estimating detector efficiencies can be summarized as:

$$\begin{aligned} \hat{\epsilon_i} &= \alpha r_i \\ r_1 &= 1 \\ r_i &= r_{i-1} \frac{T_i^{((i-1)i)mask}}{T_{i-1}^{((i-1)i)mask}}, \; 1 < i \leq n \end{aligned} \tag{11}$$

where α is a constant that is commonly chosen so that the mean efficiency is 1:

$$\alpha = \left[\frac{1}{n} \sum_{i=1}^{n} r_i \right]^{-1} \tag{12}$$

where n is the number of detectors.

III. Results

Performance of the CFSR algorithm for randoms smoothing is illustrated with phantom studies on a Biograph PET/CT (Siemens Healthcare). A 20 cm diameter cylinder activated with 1.1 mCi of ^{68}Ge was placed on the patient table low in the field of view, with two 9 cm diameter non-activated water cylinders beside it as "arms", as shown in Fig. 3. This phantom was scanned twice at each of 200, 400 and 800 sec durations, and once for 11 hours. Fig. 4 compares the measured and smoothed delayeds sinograms for the 800 sec (0.44 counts/bin) and 11 hour (22 counts/bin) acquisitions. The difference sinograms indicate there is no bias at either high or low noise levels in the data. The FSA on the other hand produces significant bias in this study, as expected (not shown).

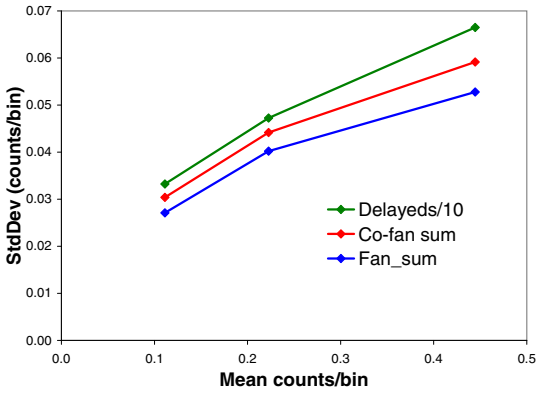

Fig. 5. Standard deviation of the noise in measured and smoothed randoms sinograms versus mean counts/bin. Note that the standard deviations of the delayed coincidence data have been divided by 10 here.

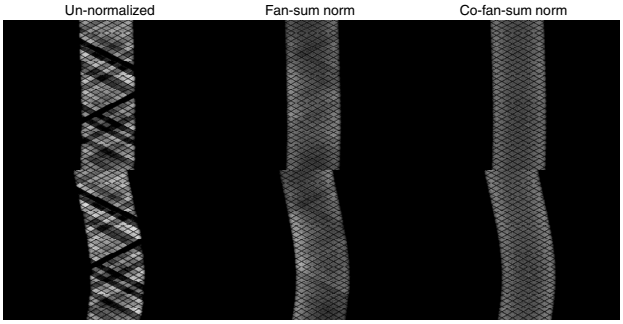

Fig. 6. Unnormalized and normalized sinograms. Top: using a centered cylinder. Bottom: using a cylinder 35 mm off-center. Global grayscale across rows.

The standard deviations of the noise of the measured and smoothed delayeds sinograms were determined from the replicate scans using the technique described in [9]. These noise estimates are shown in Fig. 5 as a function of the average counts/bin in the sinograms. Note that the standard deviations of the unsmoothed sinograms have been divided by 10 for this plot. The CFSR algorithm has about 12% higher noise than FSA, but still reduces the noise in the measured data by over a factor of 10.

Fig. 6 shows examples of the application of the CFSR algorithm to the normalization of sinograms acquired on a scanner with detectors having significant efficiency variations (the image grayscales are windowed to emphasize this variation). Two cases are shown: one with a centered 20 cm cylinder phantom, and one where the cylinder was displaced from the center of the FOV by 35 mm. The intrinsic detector efficiencies were estimated from each scan using both the CFSR algorithm and the FSA. These estimated efficiencies were then applied to the data to normalize the corresponding sinograms. In both cases the CFSR algorithm produced a more uniform normalized sinogram than the conventional FSA.

IV. Discussion

We have described a new exact analytical algorithm for estimating single event rates from delayed coincidence data. The mask-restricted CFSR algorithm can also give accurate estimates of intrinsic detector efficiencies when applied to true coincidence data from a known phantom. These estimates have low noise because they employ nearly all of the measured data. If the data are uncompressed, i.e. in native LOR format, then the estimates will be unbiased. Although we have described only the 2D implementation of the CFSR algorithm here, we have recently extended it to a 3D "co-cone-sum-ratio" (CCSR) algorithm by including all measured cross-ring as well as in-ring LORs acquired by each detector in the sums, using native LORs. Initial results are encouraging, and we expect this 3D CCSR algorithm to be competitive with maximum likelihood algorithms for randoms smoothing and detector normalization, but this remains to be quantitatively evaluated.

References

[1] C. W.Stearns *et al.*, "Random coincidence estimation from single event rates on the Discovery ST PET/CT scanner," *"2003 IEEE NSS and MIC Conf. Rec."*, 2003, M14-204.

[2] M. E.Casey and E. J.Hoffman, "Quantitation in positron emission computed tomography: 7. a technique to reduce noise in accidental coincidence measurements and coincidence efficiency calibration," *J. Comput. Assist. Tomogr.*, vol. 10, no. 5, pp. 845–850, 1986.

[3] E. J.Hoffman *et al.*, "PET system calibration and corrections for quantitative and spatially accurate images," *IEEE Trans. Nuc. Sci.*, vol. 36, no. 1, pp. 1108–1112, Feb. 1989.

[4] M.Defrise *et al.*, "A normalization technique for 3D PET data," *Phys. Med. Biol.*, vol. 36, pp. 939–952, 1991.

[5] V. Y.Panin *et al.*, "Simultaneous update iterative algorithm for variance reduction on random coincidences in PET," *"2007 IEEE NSS and MIC Conf. Rec."*, pp. 2807–2811, 2007, M12-4.

[6] L. G.Byars *et al.*, "Variance reduction on randoms from delayed coincidence histograms for the HRRT," *"2006 IEEE NSS and MIC Conf. Rec."*, pp. 2203–2205, 2006, M06-377.

[7] V. Y.Panin, "Iterative algorithms for variance reduction on compressed sinogram random coincidences in PET," *"2008 IEEE NSS and MIC Conf. Rec."*, pp. 3719–3725, 2008, M06-25.

[8] ——, "Regularization methods in iterative algorithms for variance reduction on compressed sinogram random coincidences," *"2009 IEEE NSS and MIC Conf. Rec."*, pp. 2834–2838, 2009, M05-289.

[9] C. C.Watson, "Image noise variance in 3D OSEM reconstruction of clinical time-of-flight PET," *2006 IEEE Nuc. Sci. Symp. Conf. Rec.*, vol. 53, pp. 1736–1739, 2006, M04-5.